Development and Test of a Single-Aperture 11 T Nb_3Sn Demonstrator Dipole for LHC Upgrades

A. V. Zlobin, N. Andreev, G. Apollinari, B. Auchmann, E. Barzi, R. Bossert, G. Chlachidze, M. Karppinen, F. Nobrega, I. Novitski, L. Rossi, D. Smekens, D. Turrioni, and R. Yamada

***Abstract*—The upgrade of the LHC collimation system foresees installation of additional collimators around the LHC ring. The longitudinal space for the collimators could be provided by replacing some 8.33 T NbTi LHC main dipoles with shorter 11 T Nb_3Sn dipoles compatible with the LHC lattice and main systems. To demonstrate this possibility, FNAL and CERN have started a joint program with the goal of building a 5.5 m long twin-aperture dipole prototype suitable for installation in the LHC. The first step of this program is the development of a 2 m long single-aperture demonstrator dipole with a nominal field of 11 T at the LHC nominal current of 11.85 kA and ∼20% margin. This paper describes the design, construction, and test results of the first single-aperture Nb_3Sn demonstrator dipole model.**

***Index Terms*—Accelerator magnets, large hadron collider, magnet test, superconducting coils.**

I. Introduction

THE LHC operation plans include an upgrade of the LHC collimation system [1]. Additional cold collimators will be installed in the dispersion suppression (DS) areas around points 2, 3 and 7, and high luminosity interaction regions at points 1 and 5. The required space of ∼3.5 m for the additional collimators could be provided by using 11 T dipoles as replacements for several 8.33 T LHC main dipoles (MB). These dipoles, operating at 1.9 K and powered in series with the MBs, will deliver the same integrated strength at the nominal LHC current. The operating field level requires using Nb_3Sn superconductor. Recent advances in the development of high-field Nb_3Sn accelerator magnets suggest that this technology is ready for this application.

To demonstrate feasibility, CERN and FNAL have started a R&D program to build and test a 5.5 m long twin-aperture Nb_3Sn dipole for the LHC upgrade. Two such cold masses with a cold collimator in between will replace one 14.3 m long LHC MB dipole. The program started in 2011 with the design and construction of a 2 m long single-aperture Nb_3Sn demonstrator dipole magnet with a 60 mm bore, an 11 T field at the LHC nominal current of 11.85 kA and 20% margin [2].

This paper summarizes details of the design and assembly of the single-aperture Nb_3Sn demonstrator dipole and discusses its quench performance. Results of magnetic measurements and heater studies are reported elsewhere [3], [4].

Manuscript received October 9, 2012; accepted November 13, 2012. Date of publication December 24, 2012; date of current version January 28, 2013. This work was supported by Fermi Research Alliance, LLC, under Contract DE-AC02-07CH11359 with the U.S. Department of Energy and European Commission under FP7 Project HiLumi LHC, GA no. 284404.

A. V. Zlobin, N. Andreev, G. Apollinari, E. Barzi, R. Bossert, G. Chlachidze, F. Nobrega, I. Novitski, D. Turrioni, and R. Yamada are with Fermi National Accelerator Laboratory, Batavia, IL 60510 USA (e-mail: zlobin@fnal.gov; andreev@fnal.gov; apollina@fnal.gov; barzi@fnal.gov; bossert@fnal.gov; guram@fnal.gov; nobrega@fnal.gov; novitski@fnal.gov; turrioni@fnal.gov; yamada@fnal.gov).

B. Auchmann, M. Karppinen, L. Rossi, and D. Smekens are with the European Organization for Nuclear Research, CERN CH-1211, Genève 23, Switzerland (e-mail: bernhard.auchmann@cern.ch; Mikko.Karppinen@cern.ch; Lucio.Rossi@cern.ch; david.smekens@cern.ch).

Color versions of one or more of the figures in this paper are available online at http://ieeexplore.ieee.org.

Digital Object Identifier 10.1109/TASC.2012.2236138

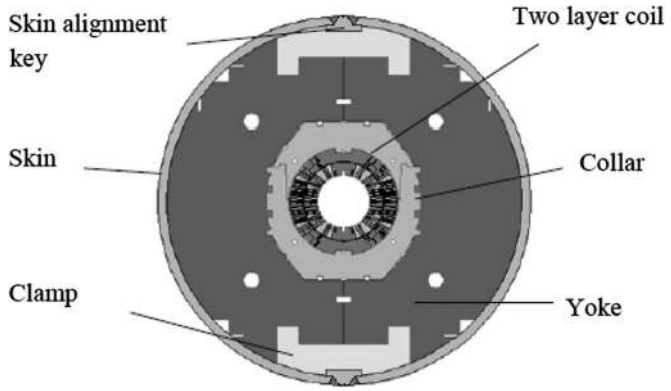

Fig. 1. Cross-sections of the cold mass.

II. Magnet Design

The design concept of the single-aperture 11 T Nb_3Sn demonstrator dipole is described in [5]. To allow for the beam sagitta in straight Nb_3Sn magnets, the coil aperture was increased to 60 mm. The coil cross-section was optimized to provide a dipole field of 11 T at the 11.85 kA current with 20% margin, and geometrical field errors below the 10^{-4} level.

The coil cross-section was designed using 15.1 mm wide and 1.29 mm thick Rutherford cable and 0.10 mm thick insulation. The 6-block coil consists of 22 turns in the inner layer and 34 turns in the outer layer separated by 0.506 mm thick interlayer insulation. The mid-plane insulation is 0.125 mm per coil. Coil end blocks were designed to reduce the field level and minimize integrated low-order field harmonics.

The cross-section of the demonstrator dipole cold mass is shown in Fig. 1. Coil pre-stress and support is provided by stainless steel collars, a vertically split iron yoke, Aluminum clamps and a thick stainless steel skin. Two thick stainless steel end plates restrict the axial coil motion.

The coil pre-stress has to be sufficient to compensate for the differences in the coil and structure thermal contractions during cool-down, and for the Lorentz forces during magnet excitation. The design of the mechanical structure and the coil pre-stress were optimized to maintain the coils under compression up to the maximum design field of 12 T and keep the coil stress below 165 MPa during magnet assembly and operation.

Magnet quench protection is provided by internal strip heaters installed between the ground insulation layers.

Fig. 2. Keystoned 40-strand cable.

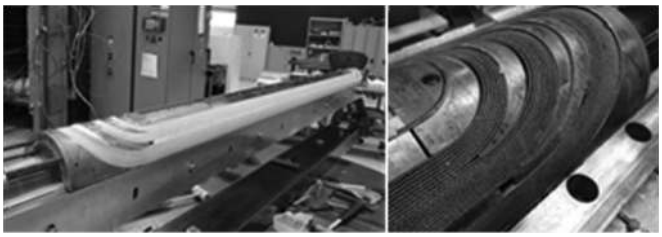

Fig. 3. Coil after curing (left) and reaction (right).

III. Magnet Construction

A. Strand and Cable

The cable was made of 0.7 mm in diameter Nb_3Sn RRP-108/127 strand with ~ 55 μm sub-elements, the nominal $J_c(12\ T, 4.2\ K) \sim 2750$ A/mm^2, the $\sim$53% Cu fraction and RRR > 60 [6]. The Rutherford cable has 40 Nb_3Sn strands, a 15 degree transposition angle and an 86% packing factor. The I_c degradation after cabling based on the extracted strand tests is $\sim$4% [7].

A 440 m long piece of cable was fabricated at FNAL providing two $\sim$210 m long unit lengths for the demonstrator dipole coils and a $\sim$25 m piece for short sample measurements. The cable was made in two steps: first with rectangular cross-section and then after annealing, it was re-rolled into the final keystoned cross-section (Fig. 2). A $\sim$220 m cable piece for a spare coil was fabricated at CERN using a one step procedure.

B. Coils, Ground Insulation, Protection Heaters

Each coil consists of two layers, 6 blocks and 56 turns. Both layers were wound from a single piece of cable insulated with two layers of 0.075 mm thick and 12.7 mm wide E-glass tape. The coil poles were made of Ti-6Al-4V alloy and wedges of stainless steel. The end spacers were also made of stainless steel using the selective laser sintering (SLS) process. The cable layer jump is integrated into the lead end spacers.

Coils were made using the wind-and-react method. During winding each coil layer was impregnated with CTD1202x liquid ceramic binder and cured under low pressure at 150 °C for 0.5 hour. During curing both coil layers were shimmed azimuthally to the same size of 1 mm smaller than the nominal coil size to prevent cable over-compression due to the Nb_3Sn cable expansion during reaction [8]. Coils were reacted separately in Argon using a 3-step cycle with $T_{max} = 640$ °C for 48 hours. Coil pictures after curing and reaction are shown in Fig. 3.

Before impregnation the Nb_3Sn coil leads were spliced to flexible NbTi cables and the coil was wrapped with a 0.125 mm thick layer of S2-glass cloth. Coils were impregnated with CTD101K epoxy and cured at 125 °C for 21 hours. The radial and azimuthal coil sizes were measured in the free condition using a 3D Cordax machine. The lengths of the coils, MBH02 and MBH03, used in the demonstrator dipole were 1965 and 1971 mm respectively including saddles and splice box.

The coil ground insulation consists of 5 layers of 0.127 mm thick Kapton film. Two quench protection heaters composed of 0.025 mm thick stainless steel strips were installed on each side of the outer coil surface. One heater was placed between the 1st and 2nd Kapton layers and the other between the 2nd and 3rd layers, covering the outer-layer coil blocks. The corresponding strips on each side of each coil were connected in serious, forming two independent heaters [4].

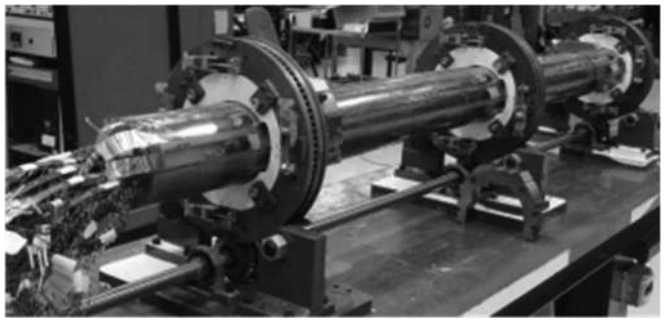

Fig. 4. Assembly of two dipole coils with protection heaters and ground insulation.

Fig. 5. Installation of collar blocks around coils (left), collared coil inside iron yoke (right).

C. Magnet Assembly and Instrumentation

Details of the magnet assembly are reported in [9].

Two coils surrounded by the ground insulation and 316L stainless steel protection shells were placed inside the laminated collars made of Nirosta high-Mn stainless steel. Assembly of two coils with protection heaters and ground insulation is shown in Fig. 4. The collar block installation around the coils is shown in Fig. 5 (left).

The collared coil is installed inside a vertically split yoke with a 400 mm outer diameter made of SAE 1045 iron and fixed with Al clamps. The yoke length is 1950 mm which practically covers the entire coil and the Nb_3Sn/NbTi lead splices. The 12.7 mm thick 304L stainless steel shell is pre-tensioned during welding to provide the coil final pre-compression. Two 50 mm thick 304L stainless steel end plates welded to the shell restrict the axial coil motion. Picture of the collared coil assembly inside the iron yoke and the collar-yoke shim is shown Fig. 5 (right).

The magnet was instrumented to monitor its parameters during assembly and test. Instrumentation includes 10 voltage taps (VT) on the inner layer and 9 voltage taps on the outer layer of each coil, 64 strain gauges (SG) on the coils, magnet shell and end bullets, and 4 resistive temperature sensors (RTD) along the magnet shell. A schematic of VT positions is shown in Fig. 6.

The coil prestress is provided by the coil midplane and radial shims installed inside the collared coil as well as the collar-yoke shims placed near the coil midplane area (see Fig. 5, right). The shim positions and sizes were defined using the FEA model

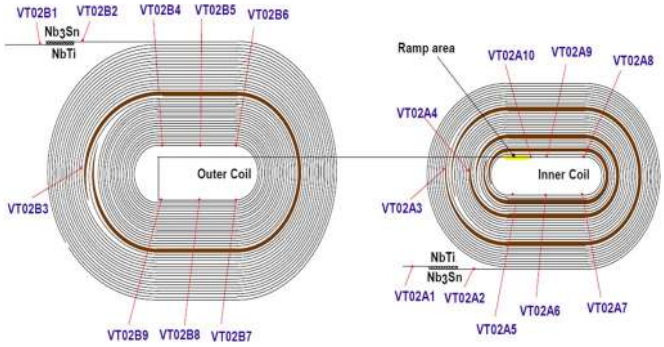

Fig. 6. Voltage tap position in inner and outer layers of the 11 T demonstrator dipole coil.

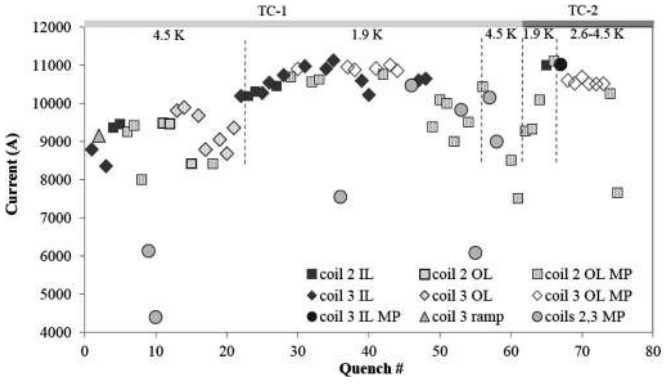

Fig. 7. Quench history and origin in TC1 and TC2.

to achieve the target coil prestress [5] and then experimentally verified and optimized by testing magnet mechanical models [10]. During magnet assembly the prestress was controlled by strain gauges installed on the coil in two cross-sections along the magnet straight section. Based on the strain gauge data the coil prestress at room temperature was close to the design values. The used instrumentation did not provide the information on coil preload after cool-down.

IV. Test Results

The 11 T demonstrator dipole (MBHSP01) was tested at Fermilab's Vertical Magnet Test Facility (VMTF) [11]. The test program included quench training and ramp rate dependence studies, magnetic measurements, and quench protection studies both at 4.5 K and 1.9 K, as well as temperature dependence and coil RRR measurements.

The quench current limit for the demonstrator dipole was estimated based on measured witness sample data. It is 13.0 kA at 4.5 K and 15.0 kA at 1.9 K, which corresponds to the bore fields of 12.3 T and 13.4 T respectively.

The magnet quench history with quench locations is summarized in Fig. 7. Magnet training started at 4.5 K with the nominal current ramp rate of 20 A/s. The first quench occurred at 8.8 kA, or 68% of the short sample limit at 4.5 K. It was originated in the coil pole turn (segment *A9_A10* in Fig. 6). However, after 5 consecutive quenches in the high field area, the quench locations moved to the outer-layer mid-plane blocks of both coils (segment *B2_B3*).

The magnet exhibited "reversed" ramp rate dependence at current ramp rates below ~60 A/s. Above this level the ramp rate dependence had a regular behavior with quenches originated practically simultaneously in the mid-plane blocks of the inner and outer coil layers (segments *A2_A3* and *B2_B3*). Similar performance was also observed at 1.9 K. Based on that the magnet quenching was continued with different current ramp rates between 40 and 70 A/s in order to reach the maximum possible quench current at both temperatures.

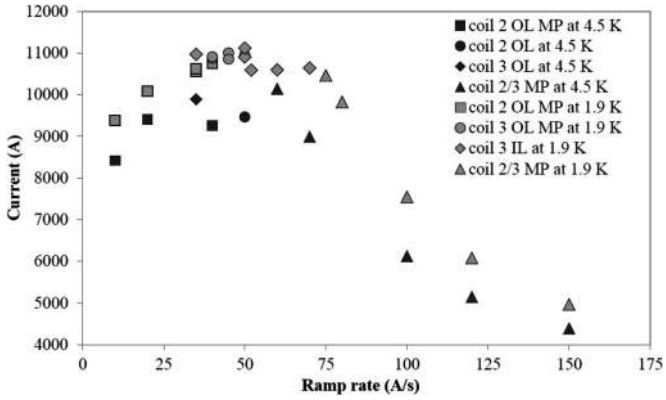

Fig. 8. Ramp rate dependence of magnet quench current at 4.5 K and 1.9 K.

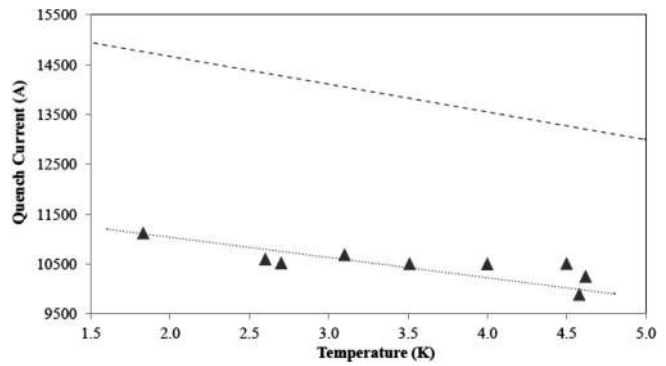

Fig. 9. Temperature dependence of magnet quench current ($dI/dt = 50$ A/s). The top dashed line represents the dependence of magnet SSL versus temperature.

Ramp rate dependences of magnet quench current at 4.5 K and 1.9 K are shown in Fig. 8. At both temperatures the magnet quench current reached its maximum at $dI/dt \sim 50 - 60$ A/s.

During the test an unplanned magnet warm-up to room temperature took place to eliminate contamination in the heat exchanger at VMTF. The magnet showed short retraining in the second thermal cycle (TC) at 1.9 K (Fig. 7). The maximum magnetic field of 10.4 T was reached at 1.9 K and a ramp rate of 50 A/s, corresponding to 78% of magnet short sample limit (SSL) at $dI/dt = 0$.

The temperature dependences of the quench current expected based on SSL calculation and measured at a ramp rate of 50 A/s (in all quenches but one at ~4.5 K) are shown in Fig. 9. The magnet demonstrates the regular temperature dependence of quench current, but also exhibits its substantial degradation and some erratic quench behavior typical of flux jump instability. All quenches at intermediate temperatures were initiated in the MBH03 outer-layer mid-plane block (segment *B2_B3*).

The observed limited quench performance could be caused by several reasons including J_c degradation and/or flux jumps in the coil outer-layer leads. Coil lead damage during magnet assembly and poor Nb_3Sn/NbTi lead splice could also explain the observed quench performance. To verify the above hypothesis several special tests were performed.

Fig. 10 shows quench current vs. holding time at current plateau at 4.5 K and 1.9 K. Magnet current was ramped to a pre-set current at 20 A/s and held until quench. Data with zero

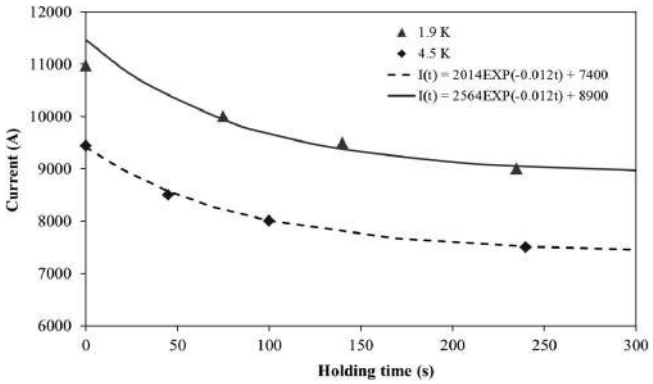

Fig. 10. Quench current at current plateau vs. holding time at 4.5 K and 1.9 K.

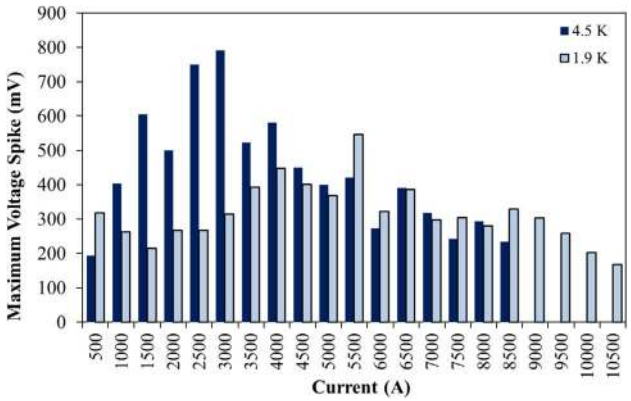

Fig. 11. Maximum spike voltage at a different current intervals.

holding time corresponds to a regular quench at 4.5 or 1.9 K at the chosen ramp rate in the range of 35–50 A/s. All holding quenches were initiated in the MBH02 outer-layer mid-plane block (segment *B2_B3* in Fig. 6). Reproducibility tests and tests at different ramp rates were not performed. Exponential fit to the experimental data suggests that the stable magnet current is about 2.5 kA and 2 kA lower than the maximum quench current reached at 50 A/s at 1.9 K and 4.5 K respectively, which is consistent with currents extrapolated to $dI/dt = 0$ on the ramp rate dependence shown in Fig. 8.

The Voltage Spike Detection System (VSDS) [12] was used to record the voltage across one coil balanced with the voltage across the opposite coil at a sampling rate of 100 kHz. The histogram in Fig. 11 shows the maximum voltage spike amplitude at different current intervals recorded during ramp up at 4.5 K and 1.9 K. Comparing these data with the data collected for other Nb_3Sn magnets made of similar RRP-108/127 strand [13], [14] one can conclude that their level is similar and much lower than in magnets made of more unstable RRP-54/61 strand [15].

A special instability suppression test, similar to that described in [14], was performed by reducing J_c in the outer-layer mid-plane area by locally heating them with protection heaters powered with a small DC current. A reduction of magnet quench current was observed. This experiment as well as modest voltage spike activity do not support the hypothesis that flux jumps are limiting quench current in the outer coil layer.

The residual resistivity ratio (RRR) of cable was measured for all segments of both coils during magnet warm-up. The average RRR value was $\sim$100 (lowest 80, highest 118). These numbers are smaller than ones measured in well-performing coils made of similar strand [14]. The splice resistance was also measured and found smaller than 2 nOhms.

V. Conclusion

The first 2 m long, single-aperture demonstrator dipole has been built and tested at Fermilab. The magnet reached 10.4 T or 78% of SSL at 1.9 K and a current ramp rate of 50 A/s showing limited quench performance. Most quenches at low ramp rates, all holding quenches and quenches at intermediate temperatures initiated in the mid-plane block of the outer coil layer. Only few training quenches occurred in the high field area at the very beginning of the test at 4.5 K and 1.9 K. Quench locations, ramp rate and temperature dependence studies, and additional tests point to the outer-layer leads in both coils limiting the magnet quench performance. Possible conductor damage in the mid-plane area during coil fabrication or magnet assembly could cause the observed degradation. The investigation of all possible causes continues, including a magnet autopsy. All appropriate changes will be implemented in the fabrication process of MBHSP02, a 1 m long dipole model of the same design, and tested.

Experimental data related to magnet quench protection and field quality were also collected during this test [3], [4] providing an important input to magnet design and performance optimization.

Acknowledgment

The authors thank the technical staff of FNAL Technical Division for contributions to magnet design and fabrication.

References

[1] L. Bottura *et al.*, "Advanced accelerator magnets for upgrading the LHC," *IEEE Trans. Appl. Supercond.*, vol. 22, no. 3, p. 4002008, 2012.
[2] A. V. Zlobin *et al.*, "Development of Nb_3Sn 11 T single aperture demonstrator dipole for LHC upgrades," in *Proc. PAC*, New York, 2011, p. 1460.
[3] G. Chlachidze *et al.*, "Quench protection study of a single-aperture 11 T Nb_3Sn demonstrator dipole for LHC," presented at the Appl. Supercond. Conf., 2012.
[4] N. Andreev *et al.*, "Field quality measurements in a single-aperture 11 T Nb_3Sn demonstrator dipole for LHC upgrades," presented at the Appl. Supercond. Conf., 2012.
[5] A. V. Zlobin *et al.*, "Design and fabrication of a single-aperture 11 T Nb_3Sn dipole model for LHC upgrades," *IEEE Trans. Appl. Supercond.*, vol. 22, no. 3, p. 4001705, 2012.
[6] M. B. Field *et al.*, "Internal tin Nb_3Sn conductors for particle accelerator and fusion applications," *Adv. Cryogenic Eng.*, vol. 54, p. 237, 2008.
[7] E. Barzi *et al.*, "Development and fabrication of Nb_3Sn rutherford cable for the 11 T DS dipole demonstration model," *IEEE Trans. Appl. Supercond.*, vol. 22, no. 3, p. 6000805, 2012.
[8] N. Andreev *et al.*, "Volume expansion of Nb_3Sn strands and cables during heat treatment," *Adv. Cryogenic Eng.*, vol. 48, no. AIP, p. 941, 2012.
[9] A. V. Zlobin *et al.*, "Status of a single-aperture 11 T Nb_3Sn demonstrator dipole for LHC upgrades," in *Proc. IPAC*, New Orleans, 2012, p. 1098.
[10] I. Novitski *et al.*, "Study of mechanical models of a single-aperture 11 T Nb_3Sn dipole," presented at the Appl. Supercond. Conf., 2012.
[11] M. J. Lamm *et al.*, "A new facility to test superconducting accelerator magnets," in *Proc. PAC*, Vancouver, Canada, 1997, p. 3395.
[12] D. F. Orris *et al.*, "Voltage spike detection in high field superconducting accelerator magnets," *IEEE Trans. Appl. Supercond.*, vol. 15, no. 2, pp. 1205–1208, Jun. 2005.
[13] R. Bossert *et al.*, "Fabrication and Test of 4 m long Nb_3Sn Quadrupole Coil Made of 114/127 RRP Strand," presented at the CEC/ICMC, Spokane, WA, Jun. 2011.
[14] G. Chlachidze *et al.*, "The study of single Nb_3Sn quadrupole coils using a magnetic mirror structure," *IEEE Trans. Appl. Supercond.*, vol. 21, no. 3, pp. 1692–1695, Jun. 2011.
[15] G. Ambrosio *et al.*, "Test results of the first 3.7 m long Nb_3Sn quadrupole by LARP and future plans," *IEEE Trans. Appl. Supercond.*, vol. 21, no. 3, pp. 1858–1862, Jun. 2011.